

Rod Frehlich*, Yannick Meillier, Michael L. Jensen, Ben Balsley
University of Colorado, Boulder, Colorado

1. INTRODUCTION

The Cooperative Atmosphere-Surface Exchange Study - 1999 (CASES-99) was conducted to investigate the atmospheric processes of the nocturnal boundary layer near Leon, Kansas (50 km) east of Wichita, Kansas during the month of October 1999 (Poulos et al. 2002). An important aspect of stable night-time turbulence is the "global intermittency" (Mahrt 1989), i.e., variations in space and time of the fine-scale turbulence quantities such as the energy dissipation rate ϵ and the temperature structure constant C_T^2 .

The statistical description of the variations in ϵ and C_T^2 are essential for valid comparison with other remote sensing techniques for estimating ϵ or C_T^2 because remote sensing estimates are produced as a spatial average of the turbulent field. The most common remote sensing measurements of ϵ include Doppler radar (Cohn 1995; Jacoby-Koaly et al. 2002) and Doppler lidar (Frehlich et al. 1998). Estimates of C_n^2 which is proportional to C_T^2 are produced by sodar (Gossard et al. 1984; Smedman 1988) and Frequency-Modulated Continuous Wave (FMCW) radar (Richter 1969; Gossard et al. 1984; Eaton et al. 1995).

The small-scale velocity statistics of turbulence were predicted for locally stationary and isotropic conditions by Kolmogorov (1941) assuming that the average energy dissipation rate ϵ was constant over a spatial domain less than the external length scale L . Kolmogorov (1962) proposed a refined similarity theory to include the random variations of ϵ . The key predictions of this theory are based on the probability density function (PDF) of ϵ as well as the spatial statistics of ϵ such as the spatial correlation and the spatial spectrum (Monin and Yaglom 1975).

In situ measurements of small scale turbulence are typically performed with fixed sensors on towers or on moving platforms such as aircraft. Both measurements are limited in their altitude coverage and aircraft provide measurements at a single altitude. In addition, to sample a given regime of spatial scale, measurements from a fast moving aircraft platform require wider bandwidth and lower noise than the same measurements from a slow moving platform (Muschinski et al. 2001).

To improve the spatial resolution of a variety of atmospheric measurements in the boundary layer, the Tethered Lifting System (TLS) was developed by the Cooperative Institute for Research in the Environmental Sciences (CIRES) at the University of Colorado (Balsley et al. 1998, 2003; Muschinski et al. 2001). A vertical array of sensors was specifically designed for the CASES-99 campaign to produce fine scale temperature and velocity measurements. These measurements could be made at fixed altitudes by keeping the platform stationary or by slowly moving the platform to produce profiles of atmospheric quantities from the surface up to an altitude of 2 km (see Fig. 1 of Balsley et al. 2003). Temperature measurements were produced with a low-frequency response solid-state temperature sensor and a high-frequency response fine cold-wire sensor. Velocity measurements were made using a sensitive Pitot-tube velocity sensor vaned into the wind and a high-frequency response fine hot-wire sensor. Both cold-wire and hot-wire signals were sampled at 200 Hz. The temperature was calibrated to an absolute accuracy better than 0.5 K and the accuracy of the linear calibration constant was better than 2%. The velocity was calibrated to an absolute accuracy of better than 1 m/s and the accuracy of the slope of the calibration curve is better than 5% (Frehlich et al. 2003). This resulting data set permits accurate spectral based estimates of the temperature and velocity structure constants (C_T^2 and $\epsilon^{2/3}$) that describe the small-scale turbulence. The sampling error of the estimates for the spectral level in the inertial range ($\epsilon^{2/3}$ and C_T^2) is typically 15% using 1 second of data. Useful turbulence measurements can be produced with time intervals as short as 0.25 s

* *Corresponding author address:* Rod Frehlich, Cooperative Institute for Research in the Environmental Sciences (CIRES), 216 UCB, University of Colorado, Boulder, CO 80309-0216; e-mail: rgf@cires.colorado.edu.

when the atmospheric variability dominates the estimation error. The statistical description of the atmospheric variability is the focus of this paper.

2. ATMOSPHERIC CONDITIONS

During the night of 20-21 October 1999 UT, a kite was chosen to loft the instruments since the winds aloft were moderate, ranging between $5\text{-}14\text{ m s}^{-1}$ over the course of the evening. Examination of earlier profiles indicates that the nocturnal jet first appeared about 0200 UT at a height of 120 m with a maximum wind speed of roughly 14 m s^{-1} , retained its general shape until just after 0715 UT, at which point wind speeds above the earlier jet peak increased to produce an almost constant profile with height up to at least 2500 m which persisted for many hours. Wind direction during this period was roughly south-southwesterly at the surface, veering gradually with increasing altitude to west-southwesterly above 150 m. The profile of wind speed and temperature is shown in Figure 1 for the time interval 8.1-8.2 UT.

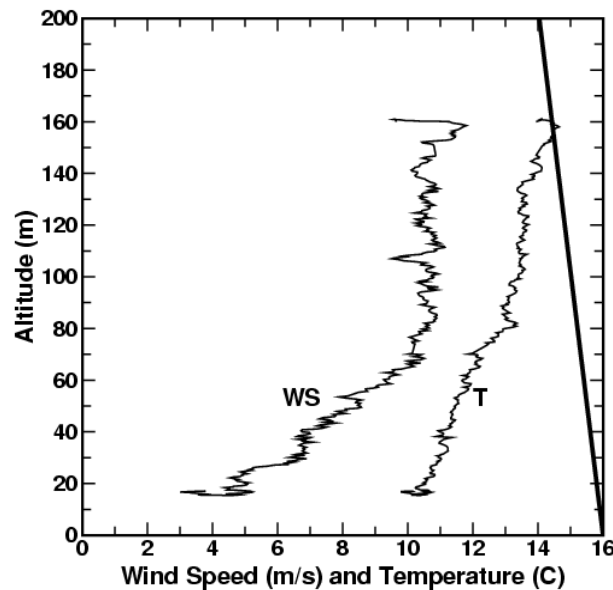


Figure 1. Wind speed and temperature vs altitude. The straight line to the right side of the plot depicts the 9.8 K km^{-1} dry adiabatic lapse rate for reference.

The profiles of energy dissipation rate ϵ and temperature structure constant C_T^2 for the same time period as Figure 1 is shown in Figure 2. The top of the boundary layer is clearly defined by the sharp drop in turbulence (ϵ and C_T^2) at an altitude of 80 m which corresponds to a slight temperature inversion and the beginning of a constant wind

speed region. Below the boundary layer height is a region of almost constant wind shear of approximately 0.13 s^{-1} . The gradient Richardson number $R_i < 0.25$ for altitudes below 80 m indicating shear generated turbulence. For altitudes above 100 m $R_i > 1$ and the potential temperature gradient is positive indicating stable conditions which is reflected in the very low values of ϵ above 100 m.

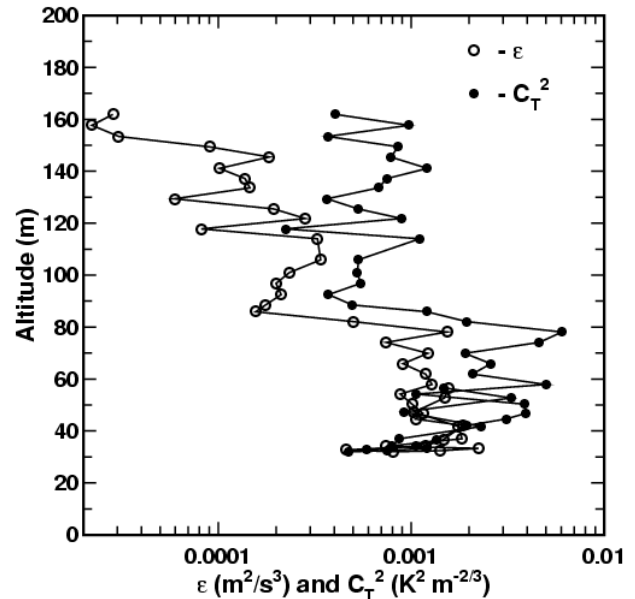


Figure 2. Small scale turbulence levels defined by ϵ and C_T^2 vs altitude for the same time interval as Figure 1.

3. SMALL-SCALE TURBULENCE ESTIMATES

Estimates of small-scale turbulence are produced from spectral estimates of the high-rate along stream velocity $u(t)$ and temperature $T(t)$ data over short time intervals. Maximum likelihood estimates (Ruddick et al. 2000) of the spectral levels are converted to ϵ and C_T^2 (Frehlich et al. 2003) assuming the small scales of turbulence are approximately isotropic with universal descriptors and assuming Taylor's frozen hypothesis (Taylor 1938) is valid which is a good approximation for the stable boundary layer (Wyngaard and Clifford 1977; Hill 1996; Frehlich et al. 2004). The velocity spectra are modeled as a universal shape which is a function of the Kolmogorov microscale. The temperature spectra are modeled as a universal shape based on the inner scale calculated from the Kolmogorov microscale. Examples of the time series of the data and spectra are shown in Figure 3 for velocity and Figure 4 for temperature at 10.54 UT and an altitude of 68.7 m. The variability

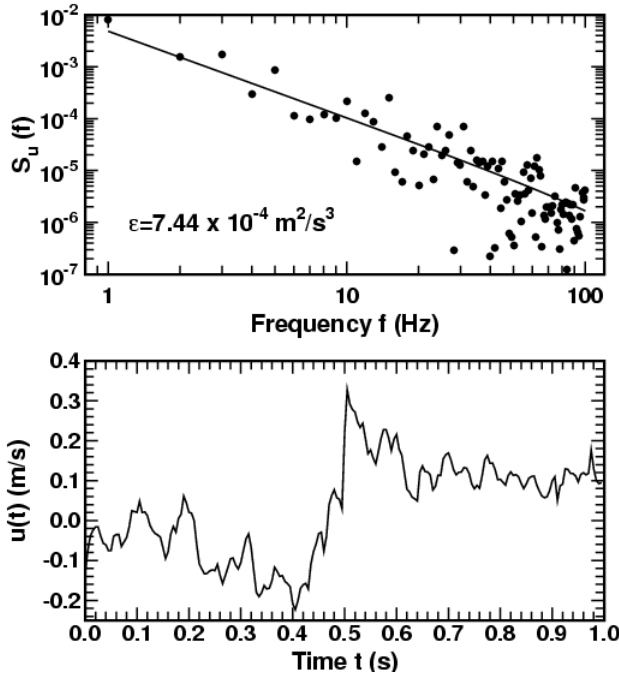


Figure 3. Time series of the along stream velocity fluctuations $u(t)$ and its spectra (\bullet) with best-fit model and estimate of ϵ .

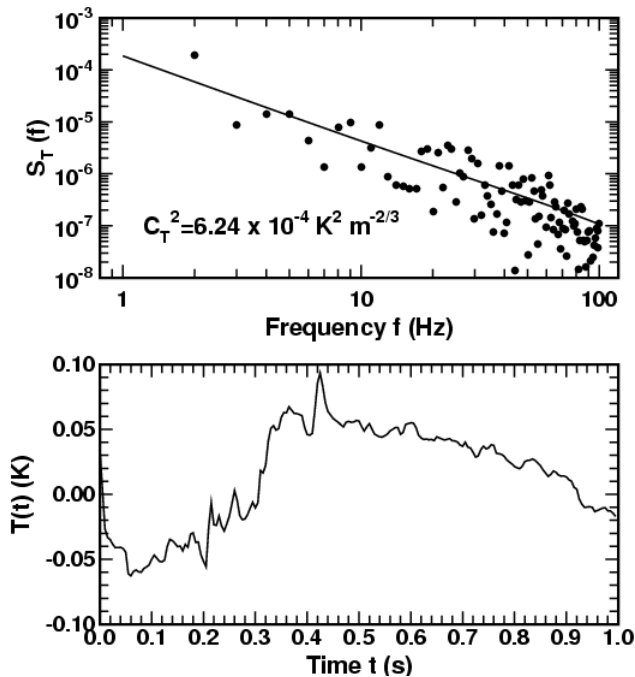


Figure 4. Time series of temperature fluctuations $T(t)$ and its spectra (\bullet) with best-fit model and estimate of C_T^2 .

of the spectral estimates is described by the exponential distribution. The accuracy of the maximum likelihood estimates of the spectral level depends on the number of useful estimates N spanning the frequency region away from the noise floor at high frequency. If one assumes half of the spectral estimates are useful then $N=50$ and the accuracy in the estimates of the spectral level is $1/N^{1/2}=0.141$.

A time series of 1-sec estimates of ϵ and C_T^2 as well as the altitude of the measurements is shown in Figure 5. The large variations in ϵ and C_T^2 are dominated by atmospheric processes since the estimation error of the measurements are less than 20%. The long period of stationarity persists over the 1.4 hours and the 10 m change in altitude because the turbulence is approximately constant with height from 60-70 m as shown in Figure 2.

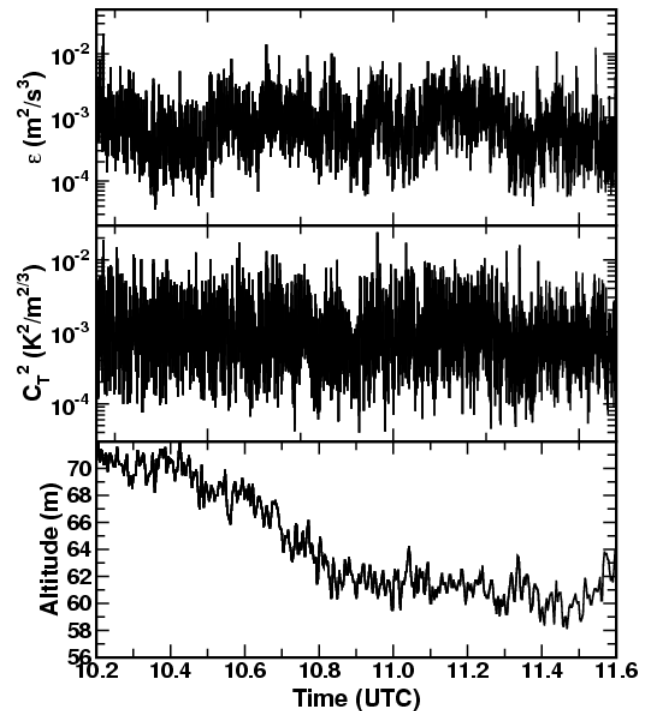


Figure 5. Time series of 1-sec estimates of ϵ and C_T^2 and the altitude of the measurements vs time.

4. STATISTICS OF TURBULENCE

The long time series of stationary turbulence estimates is essential for extracting reliable statistics of the small scale turbulence. The PDF of the 1- second estimates of ϵ and C_T^2 in Figure 5 are shown in Figures 6 and 7, respectively, as well as the predicted Gaussian distribution, i.e., a log

normal distribution for ε and C_T^2 based on the average and standard deviation of the \log_{10} of the data. The agreement is excellent for both statistics, in agreement with previous surface layer measurements (Van Atta and Chen 1970; Kukharets 1988; Bezverkhniy et al. 1986, 1988; Frehlich 1992).

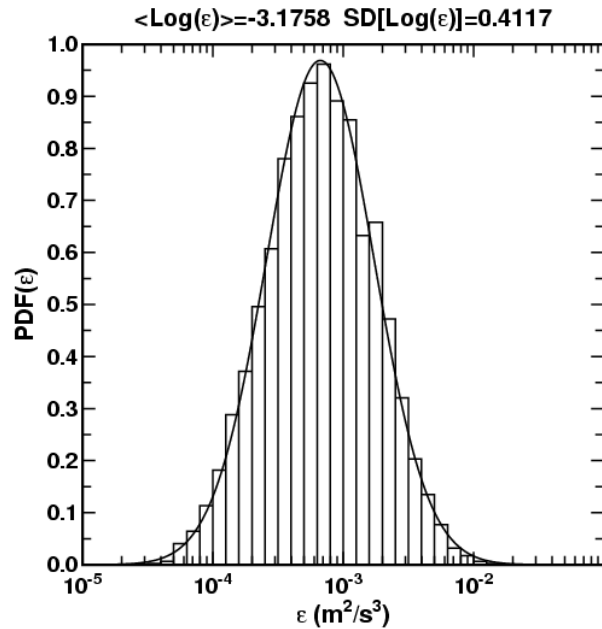


Figure 6. PDF of $\text{Log } \varepsilon$ from the data in Figure 5 and the predicted log-normal model based on the average of $\text{Log } \varepsilon$ ($\langle \text{Log } \varepsilon \rangle$) the standard deviation of $\text{Log } \varepsilon$ ($\text{SD}[\text{Log } \varepsilon]$).

Similar results are produced with estimates from 0.5 sec of data as shown in Figures 8 and 9. Note that the standard deviation of the estimates increase with decreasing measurement interval. The log normal distribution is produced for all the estimates with measurement intervals ranging from 0.25 sec to 4 sec indicating a very robust statistical description. By combing all the data from 4 packages with normalized variables (normalized by local mean and standard deviation) it can be shown that the joint PDF of ε and C_T^2 is consistent with the joint log-normal distribution (Frehlich et al. 2004).

Another important statistical description of the small scale turbulence field is the spatial spectra of ε and C_T^2 which can be estimated assuming Taylor's frozen turbulence hypothesis (Taylor 1938) to convert temporal frequency to spatial frequency. If one assumes that each measurement is equivalent to the average of the

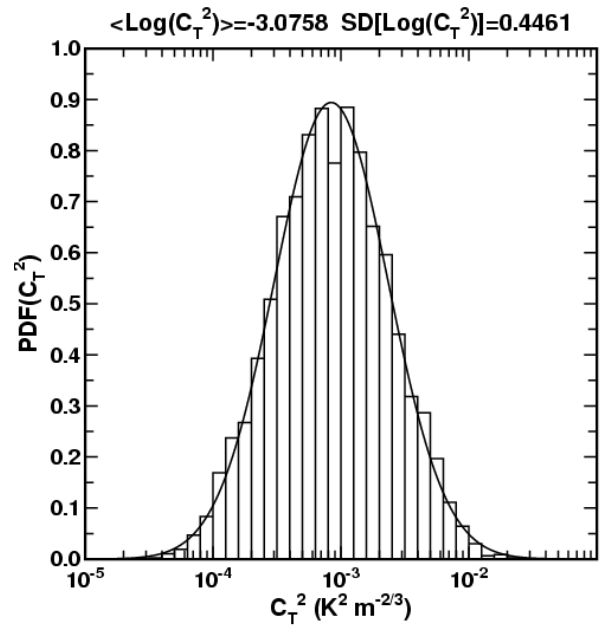


Figure 7. PDF of $\text{Log } C_T^2$ from the data in Figure 5 and the predicted log-normal model based on the average of $\text{Log } C_T^2$ ($\langle \text{Log } C_T^2 \rangle$) the standard deviation of $\text{Log } C_T^2$ ($\text{SD}[\text{Log } C_T^2]$).

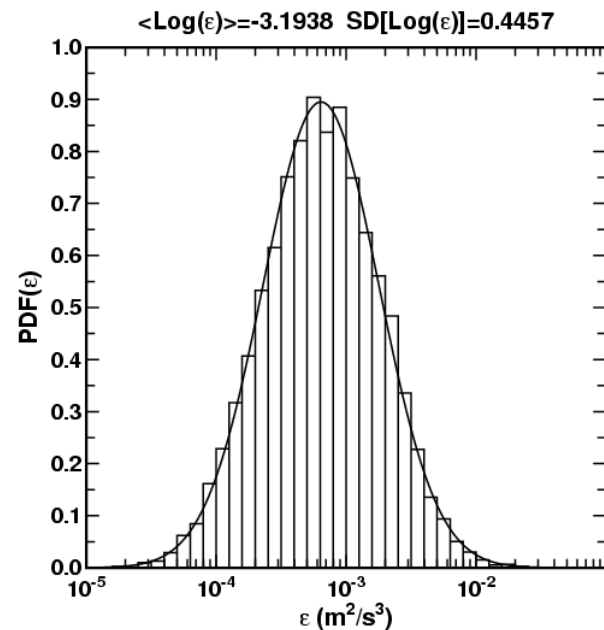


Figure 8. PDF of $\text{Log } \varepsilon$ from 0.5 sec data and the predicted log-normal model based on the average of $\text{Log } \varepsilon$ ($\langle \text{Log } \varepsilon \rangle$) the standard deviation of $\text{Log } \varepsilon$ ($\text{SD}[\text{Log } \varepsilon]$).

turbulence statistic over the observation interval T , then unbiased estimates of the spatial spectra can be produced by correcting for this averaging

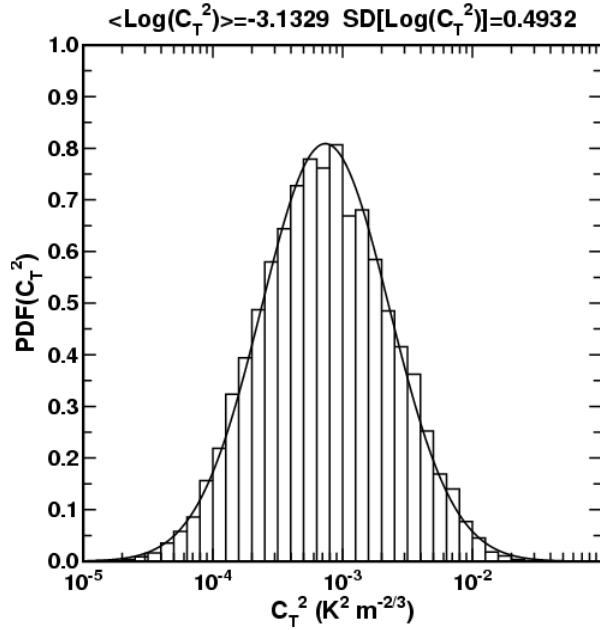


Figure 9. PDF of $\text{Log } C_T^2$ from 0.5 sec data and the predicted log-normal model based on the average of $\text{Log } C_T^2$ ($\langle \text{Log } C_T^2 \rangle$) the standard deviation of $\text{Log } C_T^2$ ($\text{SD}[\text{Log } C_T^2]$).

filter (Frehlich et al. 2004). A simple model for the spatial spectrum of the turbulence statistic x is given by

$$S_x(k) = C (L_0^{-2} + k^2)^{-\delta/2} \quad (1)$$

where $\delta = 1 - \mu$ is the slope of the spectra, μ is the intermittency exponent, and L_0 is a length scale for the fluctuations of x . The spatial spectra for ϵ and C_T^2 are shown in Figures 10 and 11, respectively, for the 0.5 second estimates. Note that the estimation error of the turbulence estimates is observed at the high frequency region of the spectra. The spatial spectrum of ϵ has $\delta \approx 0.45$ which agrees with previous results from surface layer measurements (Gibson et al. 1970; Van Atta and Chen 1970). Praskovsky and Oncley (1994) estimated $\delta \approx 0.8$ for atmospheric surface layer measurements. The spatial spectrum of C_T^2 has $\delta \approx 0.67$, a value twice as large as the $\delta \approx 0.3$ value determined by Kukharets (1988). More data is required for stationary conditions to improve the accuracy of these spectral estimates. In addition, higher bandwidth sensors would improve the accuracy of the turbulence estimates for shorter time intervals and therefore improve the high frequency region of the spectra.

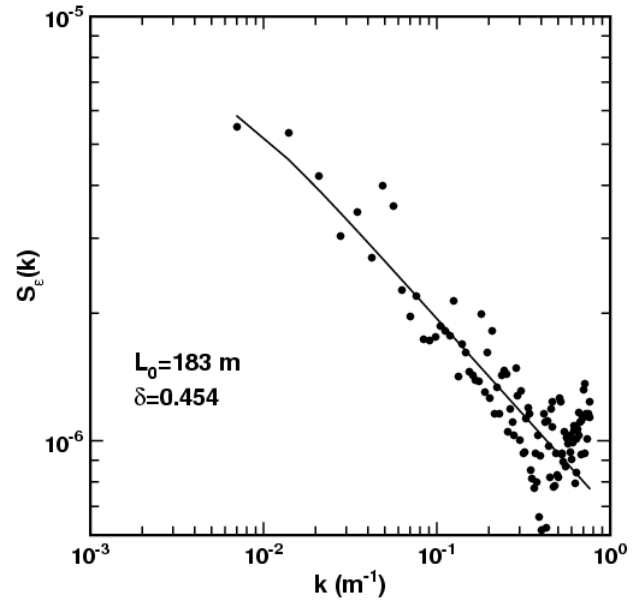


Figure 10. Spatial spectrum of ϵ (\bullet) and the best-fit to Eq. (1) (solid line).

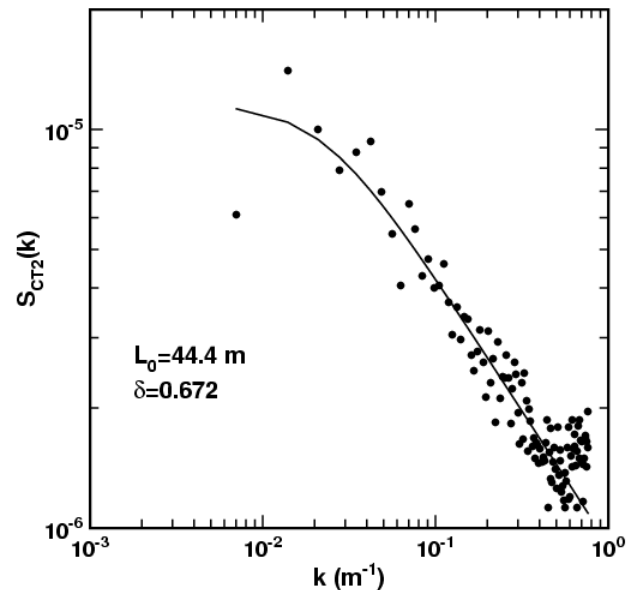


Figure 11. Spatial spectrum of C_T^2 (\bullet) and the best-fit to Eq. (1) (solid line).

REFERENCES

- Balsley, B.B., M. L. Jensen, and R. G. Frehlich, 1998: The use of state-of-the-art kites for profiling the lower atmosphere. *Bound.-Layer Meteor.*, **87**, 1-25.
- Balsley, B.B., M. L. Jensen, R. G. Frehlich, Y. Meillier, and A. Muschinski, 2003: Structure and evolution of mean and turbulence characteristics of the nighttime lower

- troposphere above Kansas in the presence of a low-level jet. *J. Atmos. Sci.*, special issue on CASES-99, **60**, 2496-2508.
- Bezverkhniy, V.A., A.S. Gurvich, and V.P. Kukharets, 1986: Variability of temperature fluctuation spectra in the atmospheric boundary layer. *Izv. Acad. Sci. USSR Atmosph. Ocean. Phys.*, **22**, 523-528.
- Bezverkhniy, V.A., A.S. Gurvich, T. I. Makarova, and M. Z. Kholmyanskiy, 1988: Variation of local temperature and wind surface speed spectra in the atmospheric surface layer. *Izv. Acad. Sci. USSR Atmosph. Ocean. Phys.*, **24**, 519-527.
- Cohn, S. A., 1995: Radar measurements of turbulent eddy dissipation rate in the troposphere: A comparison of techniques. *J. Atmos. Oceanic Technol.*, **12**, 85-95.
- Eaton, F. D., S. A. McLaughlin, and J. R. Hines, 1995: A new frequency-modulated continuous wave radar for studying planetary boundary layer morphology. *Radio Sci.*, **30**, 75-88.
- Frehlich, R., 1992: Laser scintillation measurements of the temperature spectrum in the atmospheric surface layer. *J. Atmos. Sci.*, **49**, 1494-1509.
- Frehlich, R., S. M. Hannon, and S. W. Henderson, 1998: Coherent Doppler lidar measurements of wind field statistics. *Bound.-Layer Meteor.*, **86**, 233-256.
- Frehlich, R., Y. Meillier, M. L. Jensen, Ben Balsley, 2003: Turbulence measurements with the CIRES tethered lifting system during CASES-99: calibration and spectral analysis of temperature and velocity. *J. Atmos. Sci.*, special issue on CASES-99, **60**, 2487-2495.
- Frehlich, R., Y. Meillier, M. L. Jensen, Ben Balsley, 2004: A statistical description of small-scale turbulence in the low-level nocturnal jet. *J. Atmos. Sci.*, **61**, 1079-1085.
- Gibson, C. H., G. R. Stegen, and S. McConnell, 1970: Measurements of the universal constant in Kolmogoroff's third hypothesis for high Reynolds number turbulence. *Phys. Fluids*, **10**, 2448-2451.
- Gossard, E.E., W.D. Neff, R.J. Zamora, and J.E. Gaynor, 1984: The fine structure of elevated refractive layers: Implications for over-the-horizon propagation and radar sounding systems. *Radio Sci.*, **19**, 1523-1533.
- Hill, R.J., 1996: Corrections to Taylor's frozen turbulence approximation. *Atmos. Res.*, **40**, 153-175.
- Jacoby-Koaly, S., B. Campistron, S. Bernard, B. B'enech, F. Arduin-Girard, J. Dessens, E. Dupont, and B. Carissimo, 2002: Turbulent dissipation rate in the boundary layer via UHF wind profiler Doppler spectral width measurements. *Bound.-Layer Meteor.*, **103**, 361-389.
- Kolmogorov A. N., 1941: The local structure of turbulence in incompressible viscous fluid for very large Reynolds numbers. *Dokl. Akad. Nauk SSSR*, **30**, 299-303
- Kolmogorov A. N., 1962: A refinement of previous hypotheses concerning the local structure of turbulence in a viscous incompressible fluid at high Reynolds number. *J. Fluid. Mech.*, **13**, 82-85.
- Kukharets, V. P., 1988: Investigation of variability of the structure characteristic of temperature in the atmospheric boundary layer. *Izv. Acad. Sci. USSR Atmosph. Ocean. Phys.*, **24**, 578-582.
- Mahrt, L., 1989: Intermittency of atmospheric turbulence. *J. Atmos. Sci.*, **46**, 79-95.
- Monin, A. S., and A. M. Yaglom, 1975: *Statistical Fluid Mechanics: Mechanics of Turbulence*, Volume 2. MIT Press Cambridge, MA.
- Muschinski, A., R. Frehlich, M. L. Jensen, R. Hugo, A. Hoff, F. Eaton, and B. Balsley, 2001: Fine-scale measurements of turbulence in the lower troposphere: an intercomparison between a kite-and balloon-borne, and a helicopter-borne measurement system, *Bound.-Layer Meteor.*, **98**, 219-250.
- Poulos, G. S., W. Blumen, D. C. Fritts, J. K. Lundquist, J. Sun, S. P. Burns, C. Nappo, R. Banta, R. Newsom, J. Cuxart, E. Terradellas, B. Balsley and M. Jensen, 2002: CASES-99: A comprehensive investigation of the stable

nocturnal boundary layer. *Bull. Amer. Meteor. Soc.*, **83**, 555-581.

Praskovskiy, A., and S. Oncley, 1994: Measurements of the Kolmogorov constant and intermittency exponent at very high Reynolds numbers. *Phys. Fluids.*, **6**, 2886-2888.

Richter, J.H., 1969: High resolution tropospheric radar sounding. *Radio Sci.*, **4**, 1261-1268.

Ruddick, B., A. Anis, and K. Thompson, 2000: Maximum likelihood spectral fitting: The Batchelor spectrum. *J. Atmos. Oceanic Technol.*, **17**, 1541-1555.

Smedman, A.-S., 1988: Observation of a multi-level turbulence structure in a very stable atmospheric boundary layer. *Bound.-Layer Meteor.*, **44**, 231-253.

Taylor, G. I., 1938: The spectrum of turbulence. *Proc. Roy. Soc. London*, **A132**, 476-490.

Van Atta, C. W., and W. Y. Chen, 1970: Structure functions of turbulence in the atmospheric boundary layer over the ocean. *J. Fluid Mech.*, **44**, 145-159.

Wyngaard, J.C., and S.F. Clifford, 1977: Taylor's hypothesis and high-frequency turbulence spectra. *J. Atmos. Sci.*, **34**, 922-929.